

A MORPHOLOGICAL STUDY OF POROSITY DEFECTS IN GRAPHITE-EPOXY COMPOSITES

David K. Hsu and Kevin M. Uhl

Center for NDE
Iowa State University
Ames, IA 50011

INTRODUCTION

The presence of porosity in a structural material generally has a detrimental effect on the strength and mechanical properties of the component [1]. Excessive porosity is especially undesirable in laminated composites such as graphite-epoxy as it substantially degrades the interlaminar shear strength, the compressive strength and the transverse flexural strength. Detailed morphological knowledge of the pores such as their geometrical shape, orientation and location of occurrence in the laminate is valuable in several areas. In the nondestructive evaluation of porosity in composites using ultrasound, such morphological data will aid the model development of the interaction of the ultrasonic field with the voids and help the interpretation of the ultrasonic measurement results. In the investigation of the effects of defects, data on the pore morphology serve as inputs to models of the stress distribution around the defects and the interaction between the defects.

The presence of porosity in composite laminates can be due to many causes [1,2]. Both the material constituents and the fabrication process may be contributing sources of voids. Material related causes of porosity include absorbed moisture or overaging of the prepregs, and process related causes are insufficient vacuum debulking, loss of cure pressure, and improper cure temperatures and rates. The size and shape of voids in graphite-epoxy laminates have been described in several ultrasonic studies [3,4]. Stone and Clark found that the voids tend to be small and spherical at low porosity volume fractions (less than 1.5%) and at higher volume fraction interlaminar voids due to trapped air tend to be much larger and flattened and elongated in shape. Yuhas also found that the voids are roughly cigar-shaped and increase in size with increasing volume fraction.

In this paper we report the results of an investigation on the pore morphology in graphite-epoxy laminates over a porosity volume fraction range of 0.2-6.5%. Microscopy and image analysis are used to obtain statistical data on the size, shape, orientation (relative to the laminar geometry and fiber orientation) and location of the pores. In particular, a deply technique [5], previously used for impact delamination examination, is applied to laminates containing porosity to yield morphological data in the plane of the interface. Focussed ultrasonic scanning is also

used for the location (depth) distribution of the voids. Most of the morphological data are obtained from one set of eight specimens containing 0.2-6.5% voids by volume. Because the presence of voids can be attributed to a number of causes, their morphology is also expected to depend on the constituent material properties and the curing process. For this reason, the statistical data obtained in this study may not be universal. However, most of the important morphological behaviors are found to be the same in specimens from two other sources.

EXPERIMENTAL METHODS

Samples

Three sets of graphite-epoxy laminate specimens are used in this morphological study of porosity. Most of the measurements are made on a set of eight samples made by Rohr Industries specifically to contain various amounts of porosity. Samples A1, A2, A4, and A5 are 16-ply unidirectional laminates containing, respectively, 6.51, 2.04, 1.14, and 0.2% of voids by volume according to acid digestion tests conducted by the manufacturer. Each of the acid digestion results represents an average from four locations on the panel. Samples B1, B2, B4, and B5 are 16-ply quasi-isotropic laminates with a $[+45/-45/0/90]_{2S}$ layup and containing, respectively, 4.05, 2.82, 1.25, and 0.34% voids by volume.

The second set of samples consists of thick (1/4") graphite-epoxy panels of a cross-ply layup and containing regions of low level porosity (<1%). These samples are used in the deply tests to compare the pore morphology at the ply interfaces with laminates containing higher porosity. The third set of specimens are 16-ply quasi-isotropic panels containing very low level of porosity and are used in the ultrasonic measurements to obtain the distribution in the thickness direction.

Microscopy

The principal methods used in obtaining morphological data of the pores are microscopy and image analysis. Since the pores are volumetric flaws and tend to occur at the interfaces between adjacent laminae and elongated in the direction of the fiber axis, we shall use the following convention. The "width" of a pore is the dimension of a pore cross-section (cut perpendicular to its long axis) parallel to the plies. The "height" of a pore is the dimension of a pore in a direction perpendicular to the plies. The "length" of a pore is the dimension along its long axis. To obtain statistical data on the height and width, unidirectional specimens are sectioned on a low speed diamond wafer saw (Buehler Isomet saw) perpendicular to the fiber axis. Consecutive cuts are made to produce thin slices approximately 180 μ m thick. The cutting is done at a low speed with lubricating fluid for minimum damage and the slices are cleaned briefly in an ultrasonic cleaner to remove the particles from the pores. The cleaned and dried sample slices are then examined under a stereomicroscope using both reflected light and transmitted light. (For the unidirectional samples, slices are also cut along the fiber axis and perpendicular to the plies). The same procedure is also applied to quasi-isotropic samples with the cuts made perpendicular to the fiber axis in the 0° plies. In this case the pores in the $\pm 45^\circ$ and 90° plies will be cut at an angle of 45° and 0° with respect to the long axis of the pores.

Image Analysis

Image analysis is used in obtaining the statistical data of the morphological features including the height, width, area, aspect ratio, and angle of orientation. A LeMont image analysis system with an OASYS software package is used. With the image analyzer connected to an Olympus SZH stereo light microscope, pore morphology data may be obtained by analyzing a photomicrograph of a sample slice taken with reflected light or by digitizing the cross-sectional image of the sample slice directly using the microscope. We have also deposited a thin film of gold on the sample and used the image analyzer together with a scanning electron microscope. Consistent results are obtained using the various image analysis methods.

The OASYS image analyzing software gives statistical data on the pore width, height, area, perimeter, aspect ratio, angle of orientation and their x and y coordinates. The results are given in terms of feature-by-feature data, the average, the RMS deviation, the median, and the most probable value of each quantity. In obtaining the image analysis data of the cross-sections of 16-ply laminates (2mm thick), typically five to ten 2 x 2mm frames are digitized and the results are then combined to give the statistical data.

The Deply Technique

In the deply technique (a method successfully applied in the examination of impact induced delaminations in composite laminates), the delaminations are first stained by an ether solution of gold chloride and the laminate is then partially pyrolyzed by heating in an oven. After these treatments the laminae can then be separated and the interfaces between adjacent laminae are examined. This technique works well on quasi-isotropic layup, but not the unidirectional laminates [6]. We have applied this technique to laminates containing porosity and find it very useful in revealing the pore morphology at the interfaces, especially the long pores in laminates with a void volume fraction greater than one or two percent. This technique, of course, reveals only the voids that are connected to the edges of the specimen. The deplyed surfaces, with the original void regions stained by gold, are then conveniently imaged using a SEM with its elemental analyzer tuned to the wavelength of gold. The deply method is applied primarily to obtain the pore length information. We found that, for laminates containing a few percent voids, the pores often intersect each other and form almost a networklike pattern at certain locations. The standard image analysis software is not sophisticated enough to extract the length of individual pores among the connected pattern and the lengths are therefore obtained manually by measuring them with a microscope.

RESULTS

Thin slices (180 μ m) of unidirectional graphite-epoxy laminates cut perpendicular to the fiber axis are examined microscopically using transmitted light. In this configuration only pores with a length greater than 180 μ m are visible and appear as a white region on the micrograph. Figure 1(a) shows a photomicrograph for sample A1 (6.5% voids). As can be seen, a number of voids are longer than 180 μ m and the voids occur mostly at the ply interfaces. It is also clear that most of the voids, especially the larger ones, do not have a circular cross-section. A comparison of the photomicrographs of the consecutive cuts reveals that the larger voids have rather striking length. Figure 1(b) shows a slice located 1.2mm from the slice of 1(a) and the repetition of the larger voids is clearly visible. Thin slices cut parallel to the fiber direction

often reveal needle-like void several millimeters in length or longer, depending on the void content.

To obtain the morphological data of the pore cross-section, image analysis runs are made on thicker slices (2mm) of the laminates using reflected light so that all voids are detected regardless of their length. Table 1 shows the range and the average values of the pore width and height, as defined in last section. It is found that, when the statistical ensemble is sufficiently large, the width and the height of the pore cross-section show a lognormal distribution. Qualitatively, it is easy to understand why the distribution cannot be symmetric. For example, in a sampling of pore widths with an average of $60\mu\text{m}$ there are pores several hundred micrometers wide and yet the lower limit of pore width has to be zero. Figure 2 shows a histogram for the pore width in sample A2. The lognormal distribution is demonstrated by the Gaussian distribution when the number of pores is plotted against the logarithm of the pore width. The lognormal behavior is also observed in the pore area and aspect ratio (height/width) distributions. Also shown in Table 1 is the average void aspect ratio of the laminates. (Note that the values given are for \bar{H}/\bar{W} and not \bar{H}/\bar{W}). Table 2 lists the average cross-sectional area of the voids and the percent area determined by the image analyzer. As a comparison, the volume percent determined by acid digestion is also included in Table 2. It is interesting to note that the area percent from the image analysis and the volume percent from acid digestion are reasonably close to each other for the unidirectional as well as the cross-plyed samples. This is somewhat surprising since some of the voids in the cross-plyed samples are cut at an angle by the plane perpendicular to the fibers in the 0° ply. A detailed stereological analysis for voids in composite laminates has not been done; however, empirical modeling performed on a computer shows that the orientation effect is not very important.

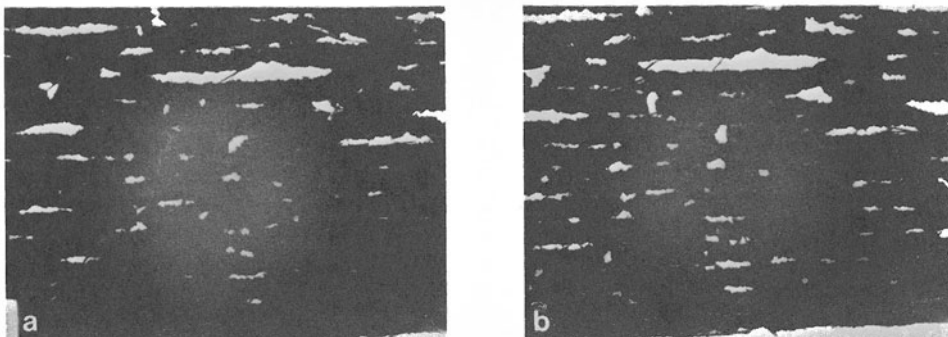


Fig. 1. Transmitted photomicrographs of a unidirectional laminate. Photos (A) and (B) are taken on two slices cut perpendicular to the fibers and separated by 1.2mm. The widths of the photos are 2.9mm.

Table 1. Distribution of porosity parameters obtained from image analysis.

Sample*	Width Range (μm)	Avg. Width (\bar{W} , μm)	Height Range (μm)	Avg. Height (\bar{H} , μm)	Avg. Ratio (\bar{H}/\bar{W})
B5	12.5-168	33.1	4.6-51.2	10.8	0.45
B4	12.8-292	56.4	4.8-47.2	15.7	0.42
B2	11.6-631	59.5	4.6-69.8	17.0	0.30
B1	11.5-995	100	4.6-72.8	19.0	0.32
A5	9.1-120	21.0	3.6-27.3	8.6	0.37
A4	10.3-137	46.4	4.1-31.3	14.4	0.36
A2	3.2-973	69.2	1.5-105	12.6	0.37
A1	1.9-896	66.4	1.1-61.9	11.2	0.32

*A's are unidirectional and B's are quasi-isotropic. Void contents are given in Table 2.

The gold staining and deply method is applied to the four cross-plyed samples (B1, B2, B4, and B5) to examine the pore morphology at the ply interfaces. Small pieces of the samples, approximately 0.4" x 0.25", are first immersed in a gold chloride solution in ether (8% gold by weight) and then heated to 800°F in an oven for about 1 hour. The plies are separated and the voids (gold stained areas) examined under a lower power stereomicroscope. Figure 3 shows the pores at the 0/90 and +45/-45 interfaces of sample B1. Because of the difficulties of picture reproduction, a trace of the photomicrograph is shown in Fig. 3. Although this technique only reveals the pores that are connected directly or indirectly to the edge of the sample, it is significant to note that there is considerable "networking" of the pores at the ply interfaces. The lengths

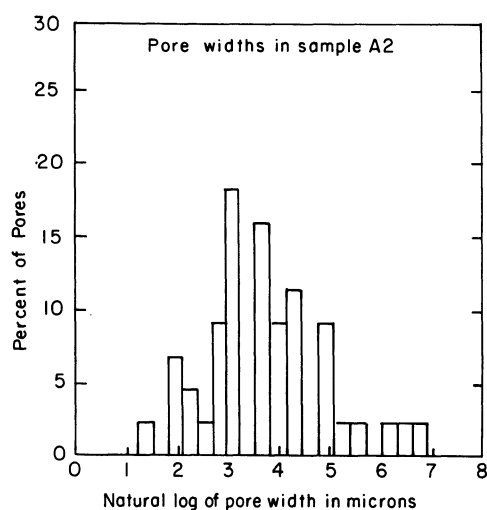


Fig. 2. Void width distribution obtained from image analysis of A2. The percentage of voids is plotted against the natural logarithm of pore width (in microns) to show the lognormal distribution.

Table 2. Average pore area and porosity area fraction from image analysis. Acid digestion results are included here for comparison.

Sample*	Average Pore Area	Area Fraction of Porosity	Volume Fraction by Acid Digestion
A5	214 μm^2	0.22%	0.20%
A4	817	1.44	1.14
A2	1650	1.77	2.04
A1	1520	7.17	6.51
B5	495	0.40	0.34
B4	1200	1.32	1.25
B2	1310	2.04	2.82
B1	2610	3.70	4.05

*A's are unidirectional and B's are quasi-isotropic.

of the pores at the 13 interfaces in samples B2, B4, and B5 are measured manually under a microscope and the length distribution are plotted. Table 3 shows the range and the average value of the pore length in each of the samples and Fig. 4 shows a histogram for sample B2. Obviously, one obtains the full length of a pore only if it is indirectly connected to the edge of the sample, but Fig. 4 serves to illustrate an approximate distribution of the pore length that is otherwise very difficult to obtain. It can also be expected that the porosity volume fraction of a sample will be dominated by the long pores since the volume of one long pore can be that of a large number of small spherical voids. Because the porosity morphology is expected to depend on material properties and curing process, the deply method is applied to a second set of samples. A thick specimen (1/4") containing approximately 1% voids is deplyed and the general behavior of the interfacial morphology is similar to the Rohr samples.

The void location distribution in the laminate thickness direction is examined both destructively with microscopy and nondestructively in a 16-ply quasi-isotropic laminate with a very low level of porosity using a focussed immersion transducer at a frequency of about 20MHz. Both visual observation and histogram plots of the y-coordinates of the pores show that the voids occur mostly at the ply interfaces. This is confirmed by an ultrasonic time of flight determination of the void depth in the low porosity specimen. Figure 5 shows the cumulative number of voids detected ultrasonically versus the pore depth. The flat regions of the curve indicate going through the interior of the plies where the cumulative number of voids does not change very much and the steeply rising regions of the curve are for the interfacial regions where most of the voids occur.

The orientation distribution of the generally elliptical pore cross-sections is also examined. The longer (width) axis of the elliptical cross-sections tends to follow the ply interface. This behavior is most prominent in higher porosity samples. Shown in Fig. 6 is a histogram showing the orientation distribution of the pores. The distribution shows a strong tendency for the flattened voids to align parallel to the plies.

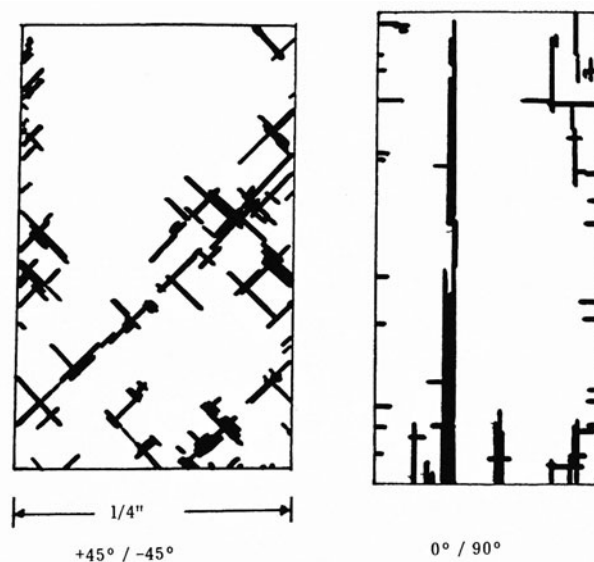


Fig. 3. Traces of two photomicrographs showing the pore morphology at the $0/90^\circ$ and $+45^\circ/-45^\circ$ interfaces of sample B1. A small piece of the laminate was first treated with a gold chloride/ether penetrant and then deplied by partial pyrolysis.

Table 3. Pore length distribution obtained on the deplied specimens.

Sample	Void Content (%)	Length range (mm)	Average Length (mm)
B5	0.34	0.1-1.7	0.38
B4	1.25	0.1-8.5	0.66
B2	2.82	0.1-10.9	1.01

Note: Lengths are based on the gold stained pores connected directly or indirectly to the edges of the specimen and 0.1mm is the resolution of the manual microscopic measurement.

SUMMARY

Detailed morphological parameters of the pores in graphite-epoxy laminates -- not only the three-dimensional shape of individual pores, but also the distribution and orientation in the multi-ply laminated composite -- are useful inputs to models of flaw-field (e.g., ultrasound) interaction and analysis of the mechanical properties. In this study, microscopy and image analysis are used to obtain statistical data on the pore morphology. A deply method is used to examine the pore morphology at the interfaces between the plies. The results confirmed the commonly accepted picture of pores occurring mostly at the ply interfaces and elongated along the adjacent fiber direction. The deply results of specimens from several different sources suggests that, although the pore morphology depends on the volume fraction and the fabrication process, the large length to width (or height) ratio seems to be a fairly common phenomenon. It also appears that the porosity volume fraction is dominated by the larger needle-like or strip crack-like pores. It is interesting

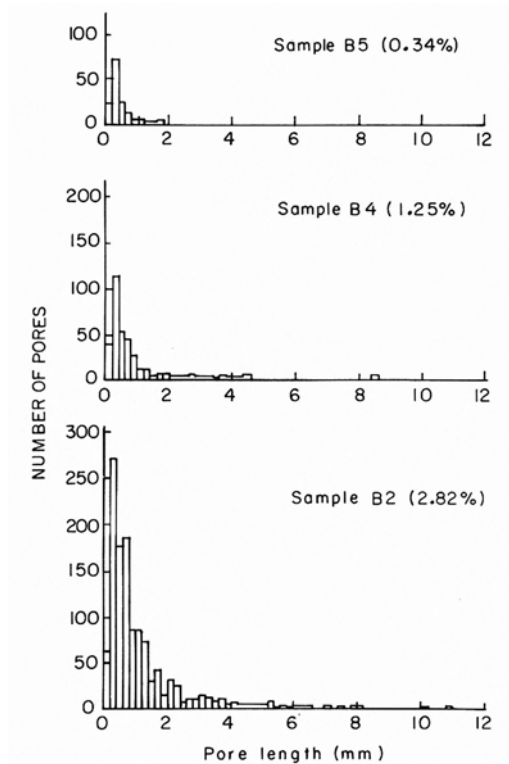


Fig. 4. Pore length distribution obtained from deplied B5, B4, and B2 samples.

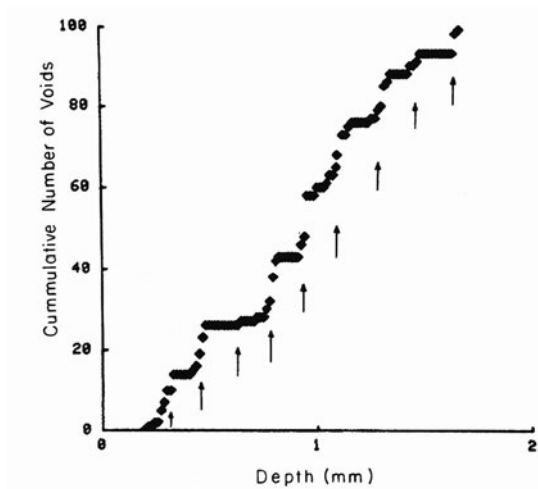


Fig. 5. Cumulative number of voids versus depth in a low level porosity sample. The voids are detected by a focussed ultrasonic beam and the depth determined by time of flight. Arrows indicate locations of ply interfaces.

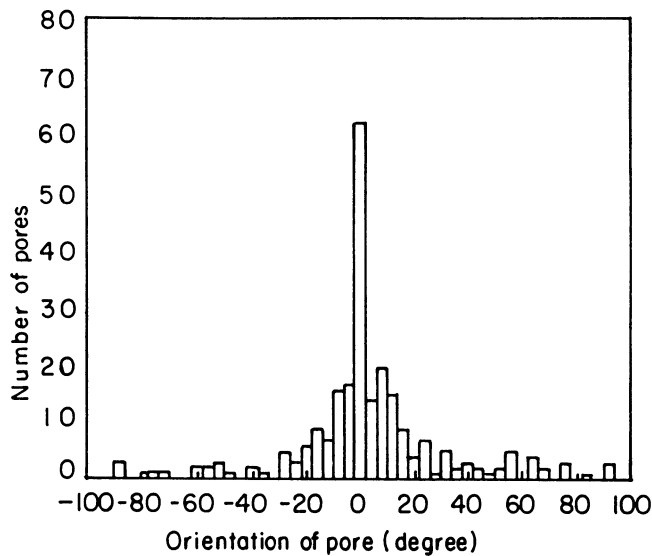


Fig. 6. Histogram of pore orientation in sample A1. Here 0° corresponds to the case where the long axis of the pore cross-section is parallel to the plies.

to note that the area fraction obtained from the image analysis of unidirectional as well as cross-plyed laminates are quite close to the volume fractions obtained by acid digestion. Finally, it should be noted that, because of the many contributing factors to the generation of porosity in graphite-epoxy composites, it is difficult to expect a universal statistical data base on pore morphology. Furthermore, since the porosity morphology is strongly influenced by the fiber layout, voids in more complex composite layups (such as laminates of woven preregs) are expected to have different morphology.

ACKNOWLEDGEMENT

This work is supported by the NSF university/industry Center for NDE at Iowa State University.

REFERENCES

1. E. M. Lenoe, "Effects of voids on mechanical properties of graphite fiber composites", AVCO Corp, Systems Division, Lowell, MA, Prepared for U.S. Air Systems Command, Rpt. AD727236 (Dec. 1970).
2. M. D. Fuller, K. A. Barrett, and R. S. Kiwak, "Production of controlled porosity specimens for ultrasonic evaluation of composite structures", in, Review of Progress in Quantitative NDE, 5B, D. O. Thompson and D. E. Chimenti, Eds., (Plenum Press, NY, 1985), pp. 1259-1269.
3. D. E. Stone and B. Clarke, "Ultrasonic attenuation as a measure of void content in carbon-fiber reinforced plastics", Nondestructive Testing, 8, 137-145 (1975).
4. D. E. Yuhas, C. L. Vores and R. A. Roberts, "Variations in backscatter attributed to porosity", in, Review of Progress in Quantitative NDE, 5B, D. O. Thompson and D. E. Chimenti, Eds., (Plenum Press, NY, 1986), pp. 1275-1284.

5. S. M. Freeman, "Correlation of x-ray radiograph images with actual damage in graphite-epoxy composites by the depley technique", Composites in Manufacturing 3 Conference, Society of Manufacturing Engineers, Dearborn, MI, 1984. Vol. EM-84, pp. 1-13.
6. E. D. Blodgett, J. G. Miller and S. M. Freeman, "Correlation of ultrasonic polar backscatter with the depley technique for assessment of impact damage in composite lamiantes", in, Review of Progress in Quantitative NDE, 5B, D. O. Thompson and D. E. Chimenti, Eds., (Plenum Press, NY, 1986), pp. 1227-1238.